ATL-TILECAL-99-020
03/11/99

ANALYSIS OF THE 1998 TEST OF THE TILECAL BARREL PROTOTYPE

V. Castillo, S. González
Instituto de Física Corpuscular (IFIC)
Universitat de València
46100 Burjassot, Spain

Abstract

The aim of this note is to report about a data analysis of the 1998 Barrel Module 0 test beam and a comparison between data and Monte Carlo simulation. The H1 weighting method has been used as an algorithm to improve the energy resolution, this method was also used for the 1994, 1996 combined tests [1] and 1997 Extended Barrel analysis [2]. The linearity and resolution of the Barrel Module 0 is simultaneously optimized and after applying H1 method there is a good agreement between the test beam data and Monte Carlo simulation. The weighting method is optimized to use only 6 parameters, plus the beam energy. Moreover the method can be used without assuming prior knowledge of the pion energy, as in a real experimental situation.

1 Test Beam Setup

The Barrel Module 0 was tested in the beam area in 1998 using the same scanning table as for the test beam in 1996. In order to improve the transverse leakage for the Barrel Module 0, the five original one meter prototype modules (old modules) were placed on either sides (in ϕ) of Module 0, three on one side and two on the other as shown in Figure 1 (left). Unlike the 1 m prototype modules, which had non-projective tower read-out, Module 0 had fibre routing such that scintillating tiles were grouped in a projective fashion with towers forming a minimun of 0.1 in η. This is shown in Figure 1 (right). This projective tower structure defined by the fibre routing in Module 0 will most likely be the projective geometry used in ATLAS. For the test beam run, only half of the module was equipped with read-out electronics (η=0 on the figure was actually the physical center of the structure).

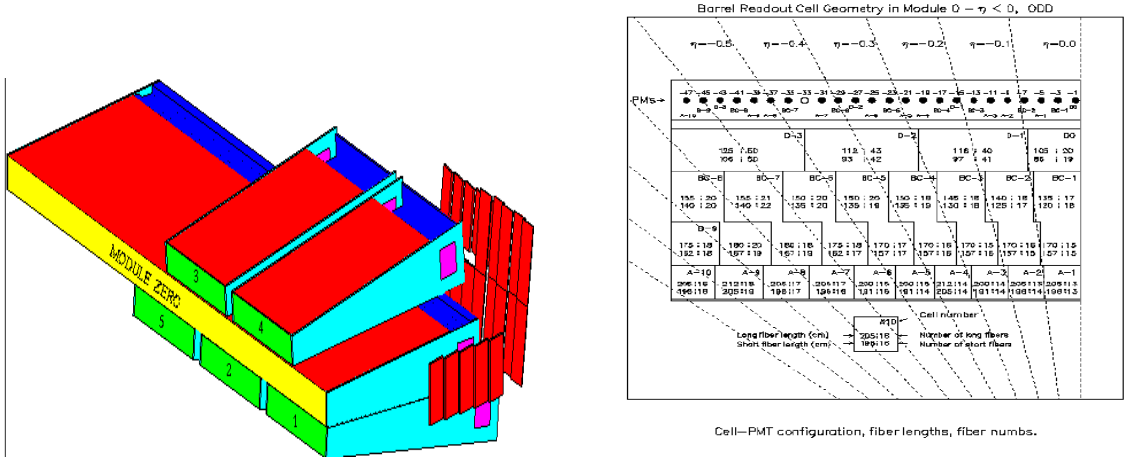

Figure 1: *Module configuration on the scanning table and Barrel Module 0 Geometry*

The Module 0 has three depth segmentations. The granularity in $\Delta\eta \times \Delta\phi$ is equal to 0.1×0.1 for the first two sampling and 0.2×0.1 for the last sampling. The thickness of the module at η=0 is 1.5 λ in the first depth sampling, 4.2 λ in the second and 1.9 λ in the third.

The electronic read-out of Module 0 was different with respect to the one used in the 1996 test beam. The two (Super) Drawers were equipped with bigain 3-in-1 readout cards into FERMI ADC modules (CAMAC ADC for the 1996 test beam). Each Super Drawer is equipped with 45 PMTs and 9 TSCs.

2. Data Sample

Pion calibration beams of different energies (20, 50, 80, 100, 150, 180, 300 and 400 GeV) at η=-0.25, -0.35, -0.45 and -0.55 have been analysed from the test beam data. On average, about ten thousand events are available for each energy. Cuts were applied in the beam chambers to eliminate the beam halo and events with simultaneous particles in the scintillator chambers; finally 60% of the events were removed including pedestal events supression.

The data obtained in the test beam has been compared with Monte Carlo simulation. The test beam setup was simulated in the framework of GEANT3.21 [3] using DICE[4,5] to simulate the geometry. The GCALOR [6] package was used to simulate the hadronic interactions. We have simulated two thousand pion events for the same energy and at different η values.

The simulation program is not complete and many features of the module 0 are not yet implemented in the simulation source code, namely:

• The fluctuations on the response of the fibers and tiles, including tile-to-tile and fiber-to-fiber fluctuactions;

• The electronics of the read-out system, including the photostatistic effect and the electronic noise effect in the response of the module 0 to the beam of particles.

3. Energy Reconstruction.

When a particle develops a shower in a block of matter such a sampling calorimeter, some fraction of its energy is transformed into a measurable signal, usually a pulse of electrical charge. This pulse is the result of all the charged particles generated in the shower development, which traverse and ionise the active layers of the detector. The energy resolution for detecting the original particle is determined by the fluctuations occuring in this process. This has consequences for calorimetric hadron detection. Firstly, the signal distribution for hadrons of energy E will be broader than for electromagnetic showers at the same energy. Secondly, the average response (signal per unit of energy) will have a different value for electromagnetic and hadronic showers $e/h > 1$.

The resolution and linearity of a non-compensated calorimeter ($e/h \neq 1$) for hadrons are degraded by the different response to the electromagnetic and hadronic components of the hadronic shower [7]. The dependence of the e/h value with the energy affects the linearity, meanwhile the presence of the electromagnetic component in the shower generated by an hadron worses the resolution. All together, to these physic effects, which are limiting the intrinsic resolution of the detector, it has to be added the always experimental contributions, basically the losses due to leakage.

The purpose of weighting techniques is to compensate for this difference and to perform the energy reconstruction optimizing the linearity and resolution. In the

present work, the evolution of the linearity and resolution parameters with the data reconstruction is studied in two steps: from raw data to H1 weighting method.

3.1 Raw Data.

The first step in the linearity and resolution study was the direct analysis of the test beam and Monte Carlo simulation raw data. The two components of the total raw energy are the energy detected in the barrel Module 0 and the energy measured in the five 1 m modules (old modules). The conversion factors from pC to GeV were calculated to be 1.26 and 36.1 for the barrel and 0.1613 and 29.2 for old modules for the test beam data and Monte Carlo simulation respectively. So finally:

$$E_{Raw} = E_{M0}^{corr} + E_{old} \tag{1}$$

Using this formula we can reconstruct the beam energy as shown in Figure 2. The mean value is similar (for the test beam data is 65.7 GeV and for the Monte Carlo simulation 65.41 GeV) but the sigma parameter is bigger in the test beam data (6.3 GeV) than in the Monte Carlo simulation (5.2 GeV). This is because the simulation program doesn't have into account the fluctuations in the response of the fibers, tiles, and because of the limited knowledge of the hadronic showers development.

According with the expresion (1) we present the results of μ, σ in table 1 for η=-0.35 and σ/μ in table 2, for four different η, obtained from the test beam data and from Monte Carlo simulation. Also the plots of linearity and energy resolution can be seen in figures 3 and 4, respectively.

η=-0.35	Test Beam data		MC simulation	
N. E. (GeV)	μ (GeV)	σ (GeV)	μ (GeV)	σ (GeV)
20	15.58±0.03	2.30±0.02	15.96±0.04	1.99±0.03
50	41.05±0.07	4.09±0.06	40.75±0.08	3.68±0.06
80	65.74±0.10	6.35±0.09	65.41±0.12	5.21±0.10
100	81.49±0.14	7.12±0.10	82.18±0.13	5.68±0.11
150	123.3±0.3	9.57±0.21	123.8±0.2	8.29±0.17
180	148.2±0.2	11.64±0.15	149.1±0.2	9.11±0.21
300	251.5±0.3	19.29±0.25	248.7±0.3	14.58±0.39
400	326.9±0.4	25.36±0.31	332.1±0.5	19.30±0.48

Table 1: *Nominal energy, mean reconstructed energy and σ at various beam energies at η=-0.35 for test beam data and Monte Carlo simulation obtained from raw data.*

The linearity pressents the typical shape of a non-compensated calorimeter, the slope is due to the increase of electromagnetic energy (π^0) with the incidente pion

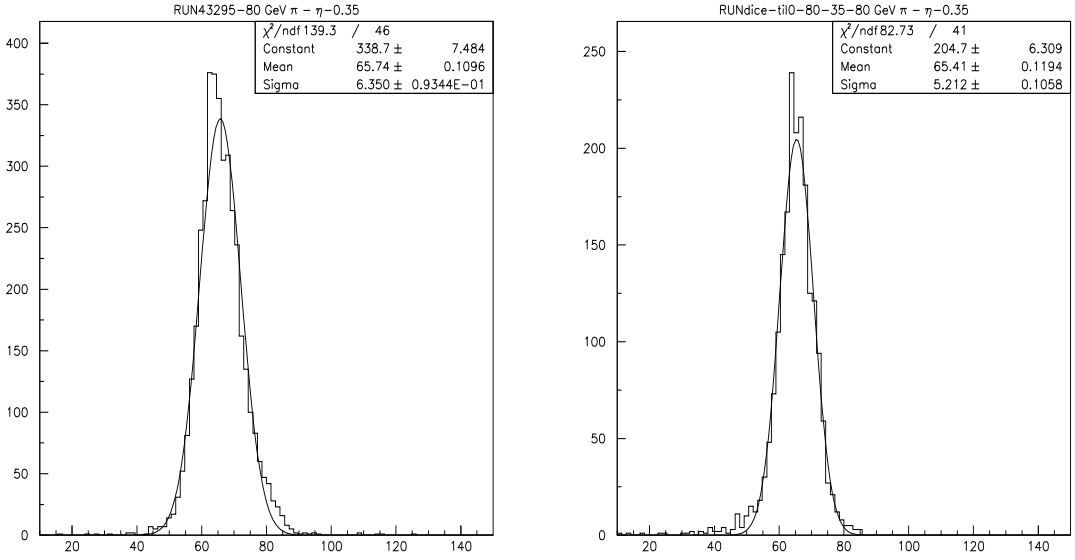

Figure 2: *Raw energy for pions at 80 GeV and η=-0.35. Left: test beam data. Right: Monte Carlo simulation.*

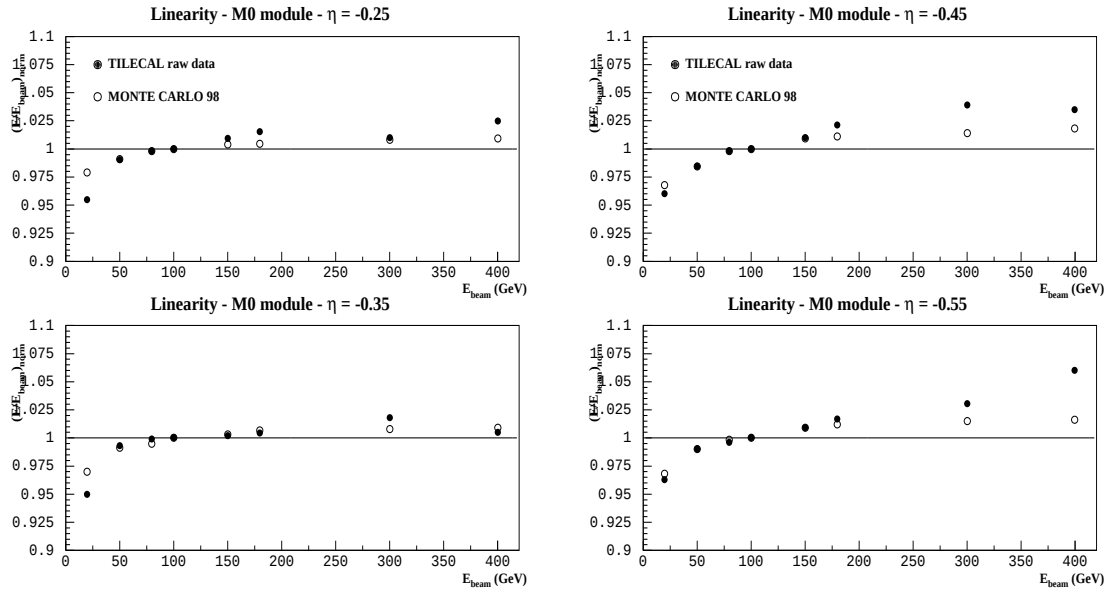

Figure 3: *Lineatiry of raw data for the test beam data and the Monte Carlo simulation. Left: for η=-0.25 (top) and η=-0.35 (bottom). Right: for η=-0.45 and η=-0.55.*

η=-0.25	Test Beam data	MC simulation
N. E. (GeV)	σ/μ(%)	σ/μ(%)
20	14.27±0.13	12.33±0.22
50	9.77±0.13	9.24±0.21
80	8.72±0.12	8.04±0.18
100	8.06±0.14	7.99±0.17
150	6.83±0.17	7.40±0.18
180	7.19±0.10	6.74±0.16
300	5.73±0.09	6.83±0.19
400	7.07±0.11	6.48±0.18
η=-0.35	Test Beam data	MC simulation
N. E. (GeV)	σ/μ(%)	σ/μ(%)
20	14.77±0.15	12.47±0.22
50	9.96±0.14	9.03±0.16
80	9.65±0.14	7.97±0.16
100	8.74±0.12	6.91±0.14
150	7.76±0.17	6.67±0.14
180	7.85±0.10	6.10±0.14
300	7.67±0.09	5.86±0.16
400	7.75±0.09	5.81±0.15
η=-0.45	Test Beam data	MC simulation
N. E. (GeV)	σ/μ(%)	σ/μ(%)
20	13.81±0.13	12.07±0.35
50	9.40±0.12	8.70±0.24
80	8.44±0.11	7.90±0.25
100	7.92±0.12	7.60±0.22
150	6.82±0.16	6.90±0.23
180	6.58±0.08	6.60±0.20
300	6.43±0.09	6.70±0.23
400	6.13±0.09	6.10±0.18
η=-0.55	Test Beam data	MC simulation
N. E. (GeV)	σ/μ(%)	σ/μ(%)
20	12.89±0.29	11.64±0.29
50	9.24±0.12	8.46±0.17
80	7.98±0.10	7.50±0.15
100	7.09±0.10	6.83±0.17
150	6.34±0.13	5.71±0.12
180	6.60±0.09	5.69±0.12
300	6.00±0.08	5.41±0.13
400	5.43±0.05	5.39±0.14

Table 2: *Nomianl energy and resolution at various beam energies at four different η for test beam data and Monte Carlo simulation obtained from raw data.*

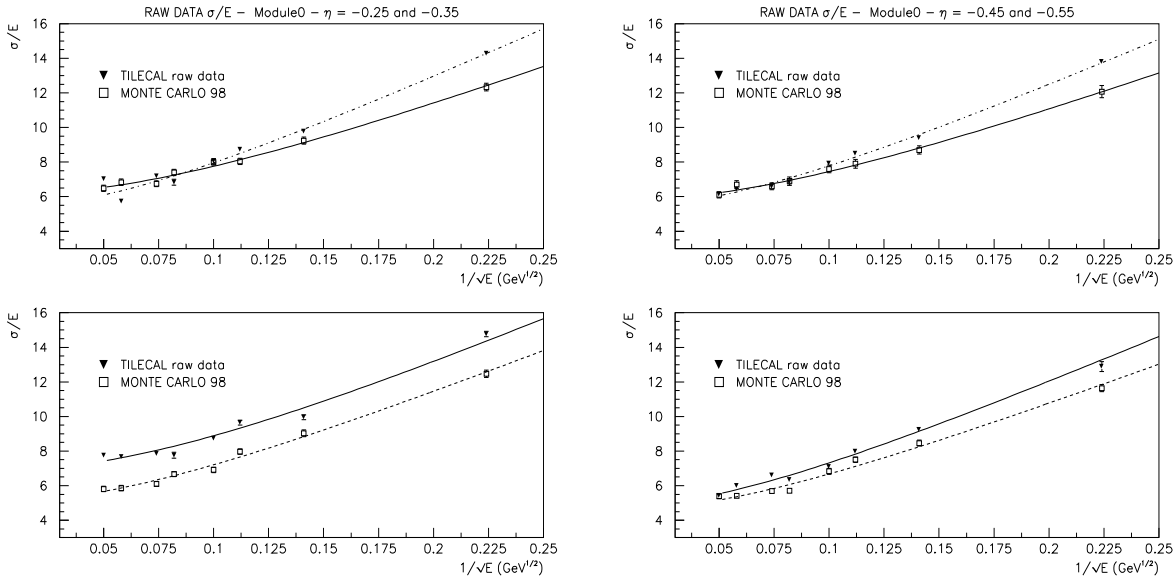

Figure 4: *Energy resolution of raw data for the test beam data and the Monte Carlo simulation. Left: for η=-0.25 (top) and η=-0.35 (bottom). Right: for η=-0.45 and η=-0.55.*

energy in the shower. The big difference between the test beam data and the Monte Carlo simulation is found at high energies. The *rms* for the test beam data is (2% for all η's) greater than for the simulation (1.3%). This is due to the data points at high energies, because the statistic is smaller in the simulation than in the data.

A fit of the data is performed in the way:

$$\frac{\sigma}{E} = \frac{\mathbf{a}\%}{\sqrt{E}} \oplus \mathbf{b}\% \oplus \frac{\mathbf{c}}{E} \tag{2}$$

where **a** represents the statistical fluctuations in the shower development, **b** is the constant term dominant at high energies and **c** is the noise term.

The fit results for the test beam data and Monte Carlo simulation are presented in the table 3.

We obtain better resolution in the simulation than in the data. The figure 2 shows that in the Monte Carlo simulation the sigma parameter is lower than for the data, therefore as the mean value is similar for both, the resolution is better in the simulation.

A study presented in a previous note [2] shows a strong correlation between parameters **a** and **c**, so that we have decided to fix the **c** value at 0.06 GeV in order to

η	Test Beam data			MC simulation		
	a (%)	b (%)	c	a (%)	b (%)	c
-0.25	59.10	5.40	0.06	48.30	6.10	0.06
-0.35	56.30	6.88	0.06	56.30	6.88	0.06
-0.45	56.50	5.35	0.06	47.30	5.75	0.06
-0.55	55.20	5.10	0.06	48.80	5.20	0.06

Table 3: *Statistical (a), constant (b), and noise (c) terms at four different η for test beam data and Monte Carlo simulation obtained from raw data.*

obtain less aleatory results in the **a** value and to compare with other fits.

3.3 H1 Method

The linearity and the resolution are two characteristics which can be improved via software offline. For that porpuse an independent approach inspired in the H1 collaboration was decided to try. Instead of correcting *upwards* the response of cells with relatively small signals, this method pretends to equalize their responses to the one of cells with large (tipically electromagnetic) deposited energies.

The energy in each cell, E_{cell}, is corrected multiplying its value by a parameter a_i [8] which depends on the energy of the cell:

$$E_{Cell}^{Cor} = a_i \times E_{Cell} \tag{3}$$

The technical details of the method have been described in ATLAS-TILECAL-NO-75. As first step, for each beam energy, the cell energy spectrum is divided into n intervals [1] and a correction parameter a_i is calculated for each interval. Several sets of parameters are calculated for all the η values and test beam data and Monte Carlo simulation, respectively.

The set of correction parameter a_i is determined from the data by minimizing the expression

$$N\ \sigma^2 = \sum_{K=1,N} (E_{cor}^K - E_{Beam})^2 + \lambda \sum_{K=1,N} (E_{cor}^K - E_{Beam}) \tag{4}$$

in which the constraint that the mean reconstructed energy has to reproduce the nominal beam energy is introduced by means of a Lagrange multiplier.

The corrected total energy spectra were fitted with Gaussian distributions over a $\pm 2\sigma$ range. From the mean values of the fits we obtain plots of the deviation

from a linear response. Such linearity plots, are shown in figure 5, left η=-0.25 ,-0.35 and right η=-0.45,-0.55, respectively. The improvement when including the "energy conservation" constraint is very clear; with this constraint, the *rms* deviation from linearity is 0.46% and 0.48% for the test beam data and Monte Carlo simulation, respectively. The two *rms* are very similar because we have reconstructed both energies minimizing the functional with the Lagrange multiplier.

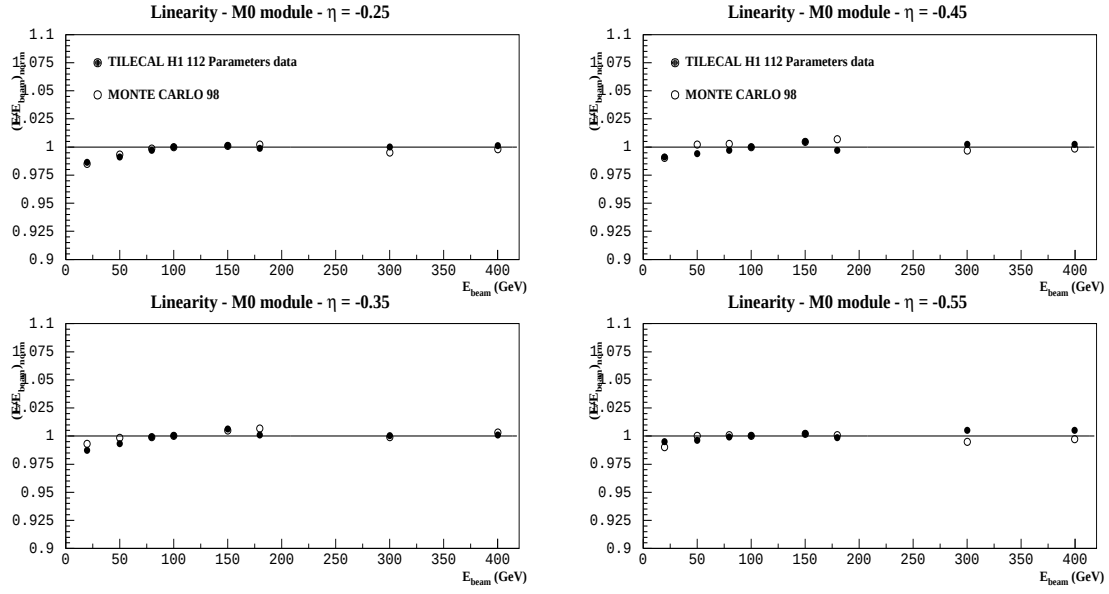

Figure 5: *Lineatiry plot minimizing the funcional with the Lagrange multiplier for the test beam data and the Monte Carlo simulation. Left: for η=-0.25 (top) and η=-0.35 (bottom). Right: for η=-0.45 and η=-0.55. The points are obtained normalizing the mean reconstructed energy values from the Gaussian fits to the value of 100 GeV.*

The results of the fits to the reconstructed pion energies are given in table 4 and 5.

The energy resolution (σ/E *vs.* the beam energy) is given in figure 6. The resolution obtained here can be parametrized for the test beam data and Monte Carlo simulation as shows the table 6.

We obtain similar resolution in the simulation than in the real data because both functional have been minimized with the Lagrange multiplier.

3.3.1 Parametrizing the a_i

A total of 112 parameters are used to reconstruct the pion energy in the Tile Calorimenter for the test beam data and Monte Carlo simulation: (13 + 1) at each

η=-0.35	Test Beam data		MC simulation	
N. E. (GeV)	μ (GeV)	σ (GeV)	μ (GeV)	σ (GeV)
20	19.87±0.05	2.11±0.05	20.10±0.04	1.98±0.03
50	50.02±0.09	3.95±0.08	50.53 ±0.08	3.77±0.07
80	80.47±0.11	5.60±0.09	80.90±0.12	5.43±0.09
100	100.7±0.1	6.80±0.10	101.2±0.1	6.24±0.12
150	152.1±0.3	9.30±0.25	153.0±0.2	9.09±0.18
180	181.4±0.2	11.10±0.16	184.2±0.3	10.75±0.22
300	302.1±0.3	18.40±0.29	303.2±0.4	16.08±0.39
400	403.1±0.4	27.40±0.45	406.0±0.7	20.80±0.48

Table 4: *Nominal energy, mean reconstructed energy and σ at various beam energies at η=-0.35 for test beam data and Monte Carlo simulation obtained with the constraint to the beam energy.*

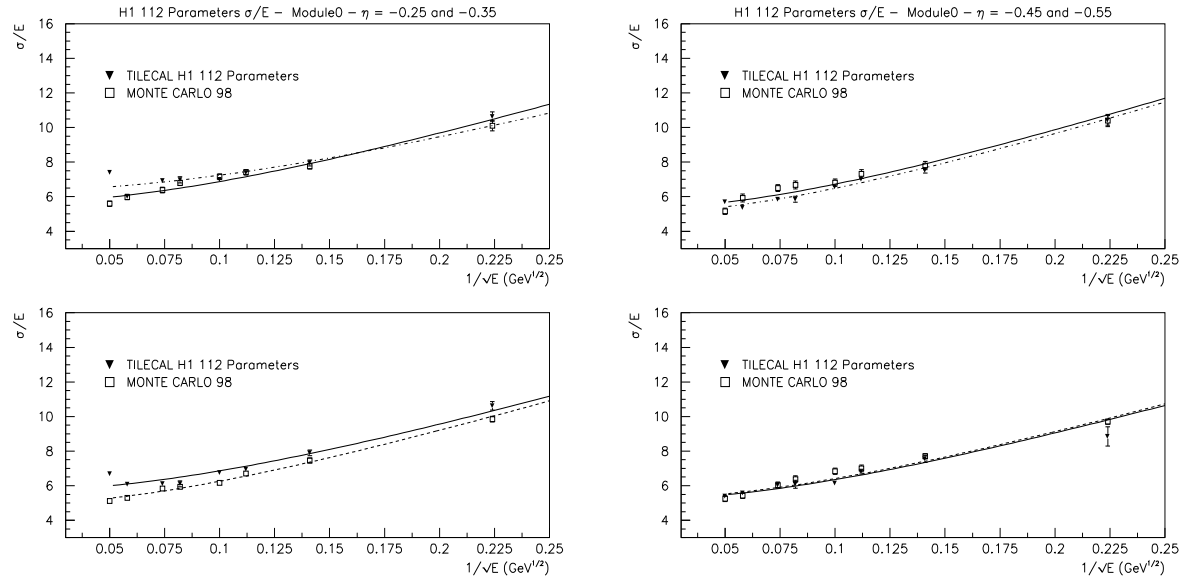

Figure 6: *Resolution plot minimizing the functional with the Lagrange multiplier for the test beam data and Monte Carlo simulation. Left: η =-0.25, (top) and η =-0.35 (bottom). Right: η =-0.45, (top) and η =-0.55(bottom) .*

η=-0.25	Test Beam data	MC simulation
N. E. (GeV)	σ/μ(%)	σ/μ(%)
20	10.63±0.27	10.10±0.29
50	7.95±0.17	7.76±0.17
80	7.39±0.13	7.51±0.16
100	6.99±0.13	7.35±0.16
150	6.98±0.18	7.09±0.15
180	6.92±0.11	6.78±0.16
300	5.93±0.11	5.98±0.15
400	7.40±0.11	5.59±0.15
η=-0.35	Test Beam data	MC simulation
N. E. (GeV)	σ/μ(%)	σ/μ(%)
20	10.62±0.25	9.85±0.27
50	7.90±0.17	7.46±0.15
80	6.95±0.12	6.71±0.12
100	6.75±0.11	6.17±0.13
150	6.11±0.17	5.94±0.13
180	6.12±0.10	5.83±0.13
300	6.09±0.09	5.30±0.13
400	6.69±0.12	5.12±0.12
η=-0.45	Test Beam data	MC simulation
N. E. (GeV)	σ/μ(%)	σ/μ(%)
20	10.41±0.28	10.40±0.27
50	7.52±0.15	7.85±0.28
80	7.00±0.11	7.31±0.29
100	6.56±0.09	6.81±0.27
150	5.85±0.17	6.70±0.24
180	5.86±0.09	6.50±0.19
300	5.36±0.07	5.92±0.25
400	5.75±0.10	5.16±0.14
η=-0.55	Test Beam data	MC simulation
N. E. (GeV)	σ/μ(%)	σ/μ(%)
20	8.85±0.49	9.70±0.15
50	7.55±0.15	7.70±0.17
80	6.81±0.11	7.06±0.19
100	6.14±0.09	6.81±0.18
150	6.08±0.19	6.78±0.19
180	6.03±0.09	6.63±0.18
300	5.58±0.09	5.42±0.16
400	5.40±0.07	5.25±0.17

Table 5: *Nominal energy and resolution at various beam energies at four different η for test beam data and Monte Carlo simulation obtained with the constraint to the beam energy.*

η	Test Beam data			MC simulation		
	a (%)	b (%)	c	a (%)	b (%)	c
-0.25	35.10	6.30	0.06	39.30	5.10	0.06
-0.35	38.40	5.60	0.06	38.90	4.90	0.06
-0.45	41.30	5.00	0.06	41.70	5.30	0.06
-0.55	37.20	5.10	0.06	37.50	5.55	0.06

Table 6: *Statistical (a), constant (b), and noise (c) terms at four different η for test beam data and Monte Carlo simulation obtained with the constraint to the beam energy.*

of the 8 beam energies. To reduce the number of parameters we proceed as follows:

• The a_i are parametrized as a function of the cell energy in the way: $y = p_1 + p_2/E_{cell}$ (with different values p_1, p_2 for the test beam data and Monte Carlo simulation). The results are shown in figure 7 for test beam data and 8 for Monte Carlo simulation for various beam energies and η=-0.45. We have applied the same prametrization and we have obtained similar results for the other η values.

The errors on the a_i shown in the figure are the *rms* values of ten independent sets of a_i obtained by classifying the data in 10 independent subsamples at each energy and solving the minimization equations for each set.

• Next, the parameters p_1, p_2 and B (the old modules parameter) are expressed as a fuction of the beam energy using simple two parameter dependence. This is shown in figures 9 and 10; for the test beam data and Monte Carlo simulation at η=-0.45. We have obtained the same behaviour for the several η's.

Following theses parametrizations, we have expressed the entire set of corrections by two sets of simple functions, containing a total of only six parameters. The aim now is to check whether the energies reconstructed with 6 rather than 112 parameters are less precise. The mean, σ for η=-0.35 and resolution values for four η obtained from this parametrization of the a_i are given in the table 7 and 8; the linearity and resolution plots are in figure 11 and 12. Comparing to the results previously obtained with 112 parameters one can see that despite the dramatic reduction of correction parameters the resolution is negligibly worse.

The linearity has degraded because the energy reconstruction is not good enough. This is due to the fact that the errors on the a_i, p_1, p_2 and B (the old modules parameter) are big, therefore these parameters could have different values than the obtained in the fit. Quantitatively, the *rms* deviation from linearity is now $\sigma = 1.19\%$ and 0.95% for the test beam data and Monte Carlo simulation, respectively, instead of 0.46% and 0.48%.

The resolution is now parametrized for the test beam data and Monte Carlo simulation as shows the table 9.

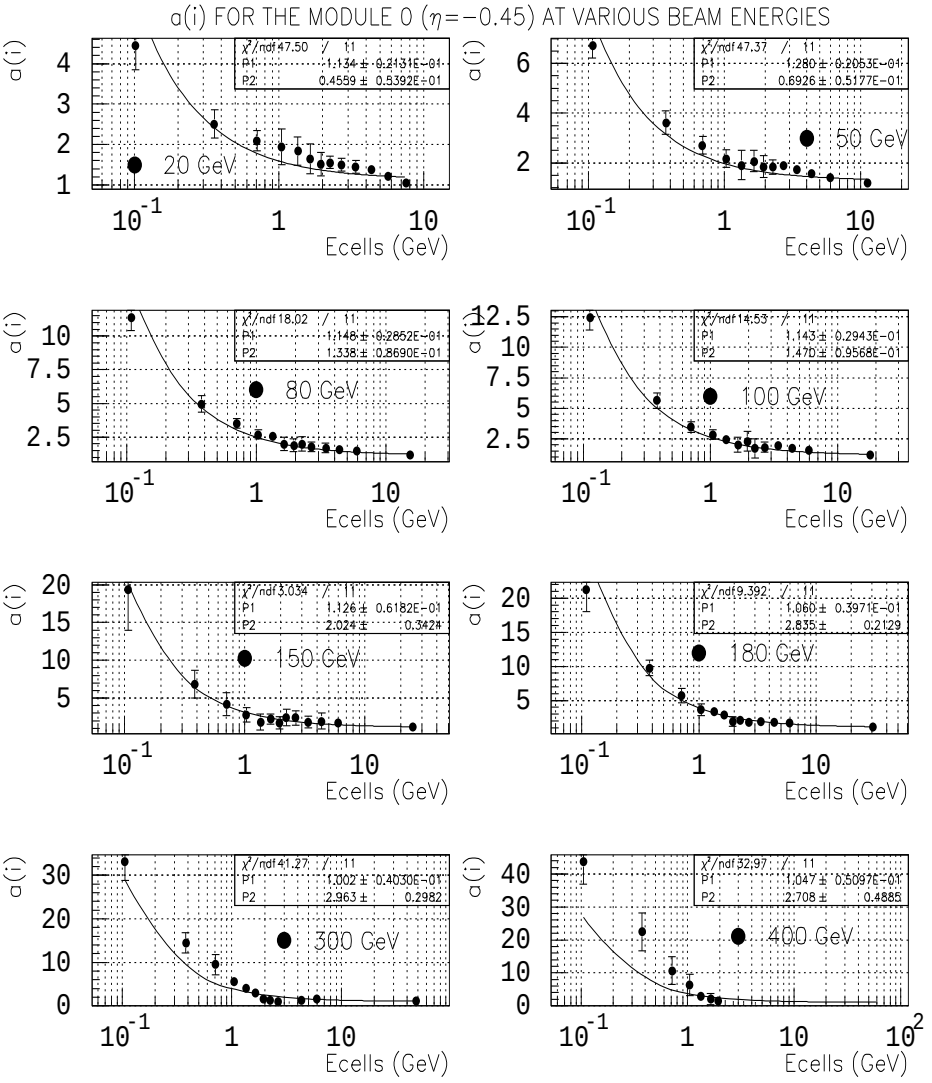

Figure 7: *Fits for the a_i parameters at various beam energies and η=-0.45 for the test beam data. The parameters p_1 and p_2 obtained are also shown on the plots.*

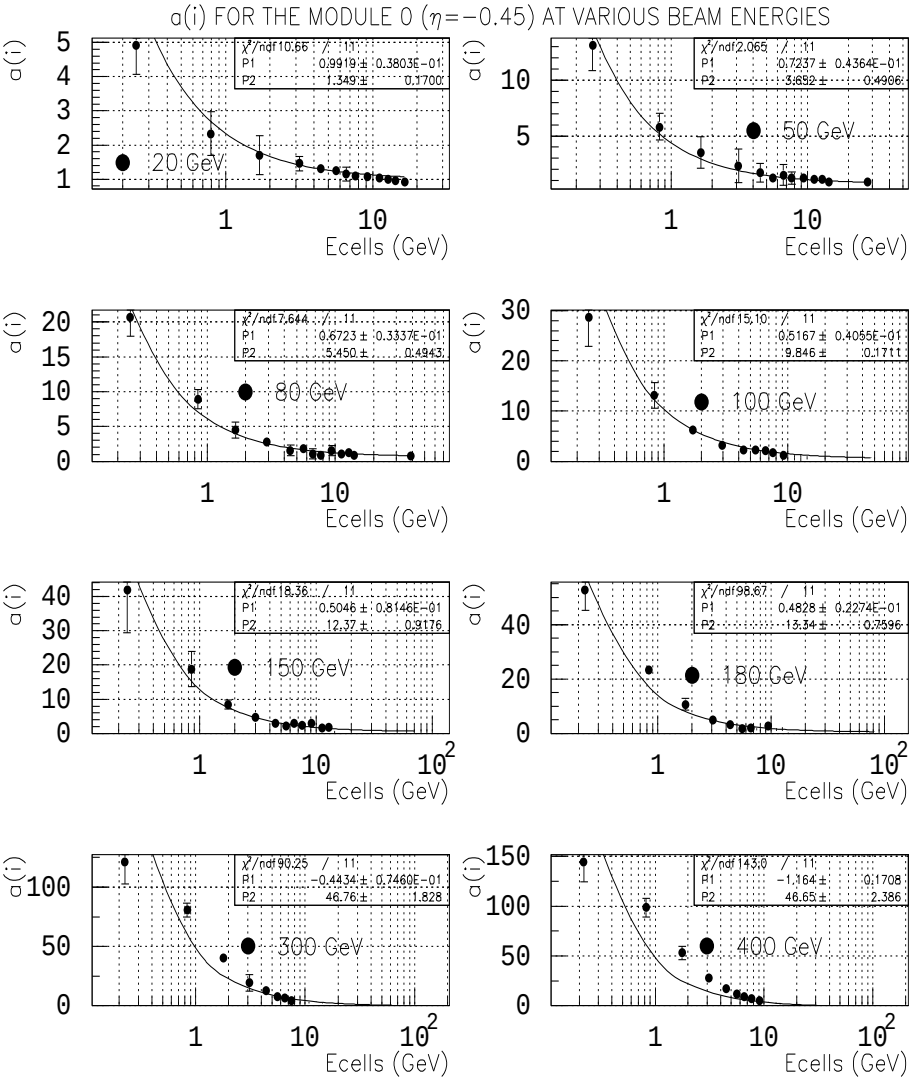

Figure 8: *Fits for the a_i parameters at various beam energies and η=-0.45 for the Monte Carlo simulation. The parameters p_1 and p_2 obtained are also shown on the plots.*

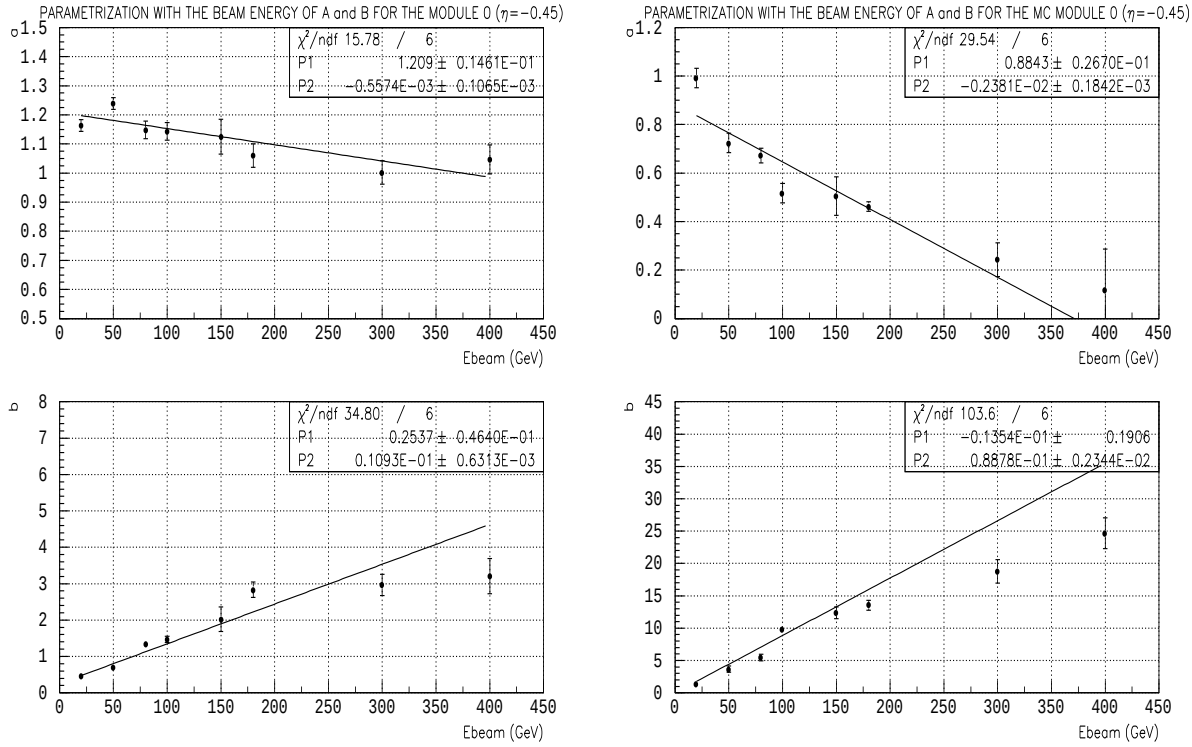

Figure 9: *For η=-0.45, the top plots show the parametrization with the beam energy of a for the test beam data (left) and Monte Carlo simulation (right) modules; the bottom plots shown the same for b. The values of the parameters from the fits are also presented on the plots.*

η=-0.35	Test Beam data		MC simulation	
N. E. (GeV)	μ (GeV)	σ (GeV)	μ (GeV)	σ (GeV)
20	19.56±0.06	2.27±0.06	20.71±0.05	2.09±0.04
50	50.23±0.09	3.95±0.08	51.22 ±0.09	3.82±0.07
80	81.50±0.11	5.68±0.09	80.10±0.12	5.19±0.09
100	101.3±0.1	6.83±0.11	98.62±0.14	5.99±0.12
150	154.5±0.3	9.19±0.24	148.3±0.2	8.21±0.16
180	185.1±0.2	10.94±0.17	178.6±0.2	9.08±0.18
300	310.4±0.3	17.74±0.28	298.2±0.6	14.08±0.49
400	405.4±0.5	26.18±0.44	396.7±0.9	16.91±0.65

Table 7: *Nominal energy, mean reconstructed energy and σ at various beam energies at η=-0.35 for test beam data and Monte Carlo simulation obtained after the parametrization.*

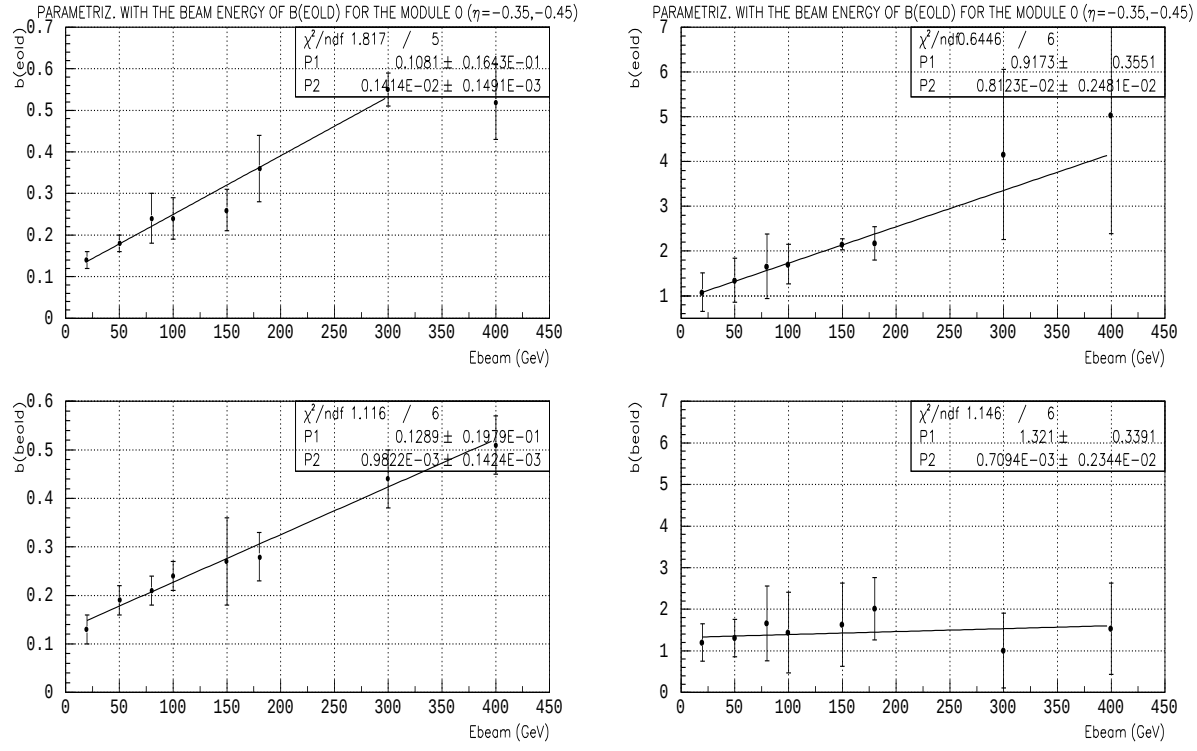

Figure 10: *The top plot show the parametrization with the beam energy of B for η=-0.35; the bottom plots show the same for η=-0.45. On the left test beam data and on the right Monte Carlo simulation. The values of the parameters from the fits are also presented on the plots.*

η=-0.25	Test Beam data	MC simulation
N. E. (GeV)	σ/μ(%)	σ/μ(%)
20	11.44±0.34	10.32±0.19
50	8.11±0.16	8.00±0.15
80	7.20±0.12	6.84±0.13
100	6.65±0.11	6.81±0.13
150	6.40±0.16	6.73±0.13
180	6.73±0.09	6.23±0.12
300	5.64±0.10	6.01±0.20
400	6.13±0.08	5.16±0.40
η=-0.35	Test Beam data	MC simulation
N. E. (GeV)	σ/μ(%)	σ/μ(%)
20	11.54±0.35	10.00±0.14
50	7.86±0.17	7.41±0.13
80	6.97±0.11	6.47±0.12
100	6.75±0.12	5.95±0.11
150	5.95±0.15	5.55±0.10
180	5.92±0.10	5.08±0.13
300	5.71±0.09	4.72±0.16
400	6.45±0.11	4.26±0.18
η=-0.45	Test Beam data	MC simulation
N. E. (GeV)	σ/μ(%)	σ/μ(%)
20	11.93±0.38	10.32±0.29
50	7.80±0.17	7.98±0.25
80	6.86±0.11	7.33±0.31
100	6.27±0.09	6.47±0.47
150	5.25±0.13	6.40±0.59
180	5.33±0.08	6.36±0.29
300	4.86±0.08	5.14±0.30
400	5.36±0.13	4.79±0.25
η=-0.55	Test Beam data	MC simulation
N. E. (GeV)	σ/μ(%)	σ/μ(%)
20	11.59±0.72	9.81±0.15
50	7.82±0.18	7.36±0.34
80	6.89±0.10	7.23±0.20
100	6.26±0.09	7.21±0.24
150	6.50±0.20	6.52±0.40
180	5.79±0.09	6.17±0.25
300	5.55±0.10	5.48±0.21
400	5.11±0.08	5.29±0.22

Table 8: *Nominal energy and resolution at various beam energies at four different η for test beam data and Monte Carlo simulation obtained after the parametrization.*

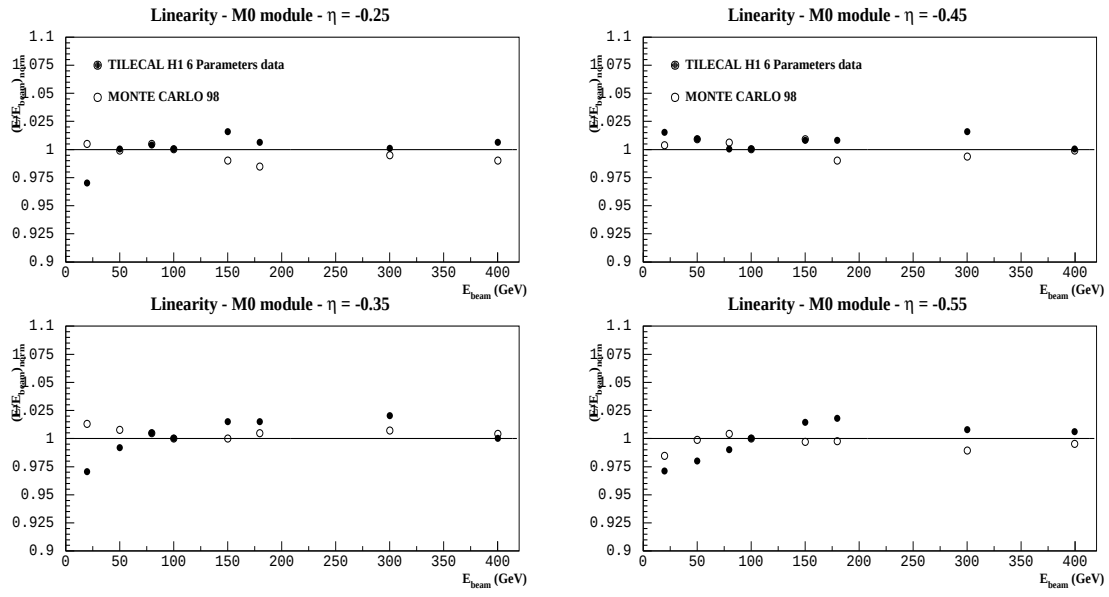

Figure 11: *Linearity after the parametrization with the beam energy for test beam data and Monte Carlo simulation. Left: For η=-0.25 (Top) and η=-0.35 (Bottom). Right: For η=-0.45 (Top) and η=-0.55 (Bottom).*

η	Test Beam data			MC simulation		
	a (%)	b (%)	c	a (%)	b (%)	c
-0.25	41.30	5.60	0.06	37.80	5.50	0.06
-0.35	41.10	5.30	0.06	42.20	3.90	0.06
-0.45	45.10	4.10	0.06	43.00	4.60	0.06
-0.55	43.40	4.70	0.06	37.70	5.10	0.06

Table 9: *Statistical (a), constant (b), and noise (c) terms at four different η for test beam data and Monte Carlo simulation obtained after the parametrization.*

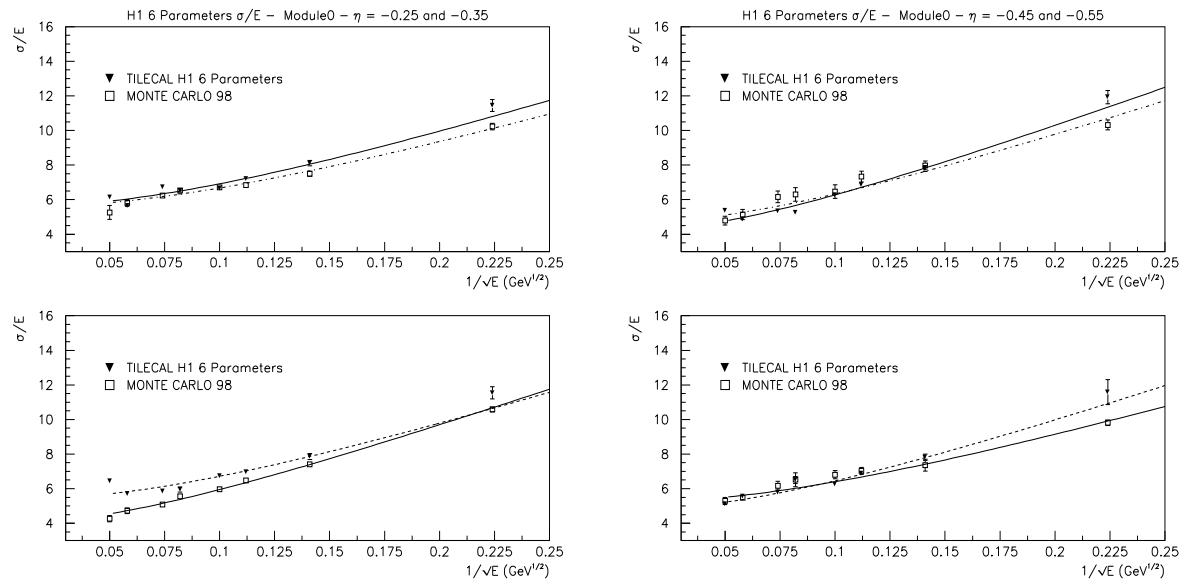

Figure 12: *Resolution after the parametrization with the beam energy for test beam data and Monte Carlo simulation. Left: For η=-0.25 (Top) and η=-0.35 (Bottom). Right: For η=-0.45 (Top) and η=-0.55 (Bottom).*

The *rms* obtained for the Monte Carlo simulation is less than for the test beam data. The drastic reduction from 112 to 6 parameters only represents an increase of 0.2 in the *rms*, both for Monte Carlo simulation and real data. For the resolution the statistical term from the fit is less in the Monte Carlo simulation than in the test beam data, this is because the resolution at low energy, where this term dominates, is better for the simulation than for the data.

3.3.2 Realistic energy reconstruction assuming no knowledge of the beam energy

The method described above cannot be used just "as it is" because the particle energy (needed to calculate the correction parameters) is unknown in a real life experiment. The aim of this section is to reconstruct the pion energy assuming no knowledge of the beam energy. A more realistic energy reconstruction can be done by obtaining an initial estimate of the particle energy from the raw data and using this estimate as a first approximation of the true energy; the procedure [2] may be iterated until it converges.

Now, we can reconstruct the energy using only 6 parameters and assuming no knowledge of the beam energy. This is shown in Figure 13

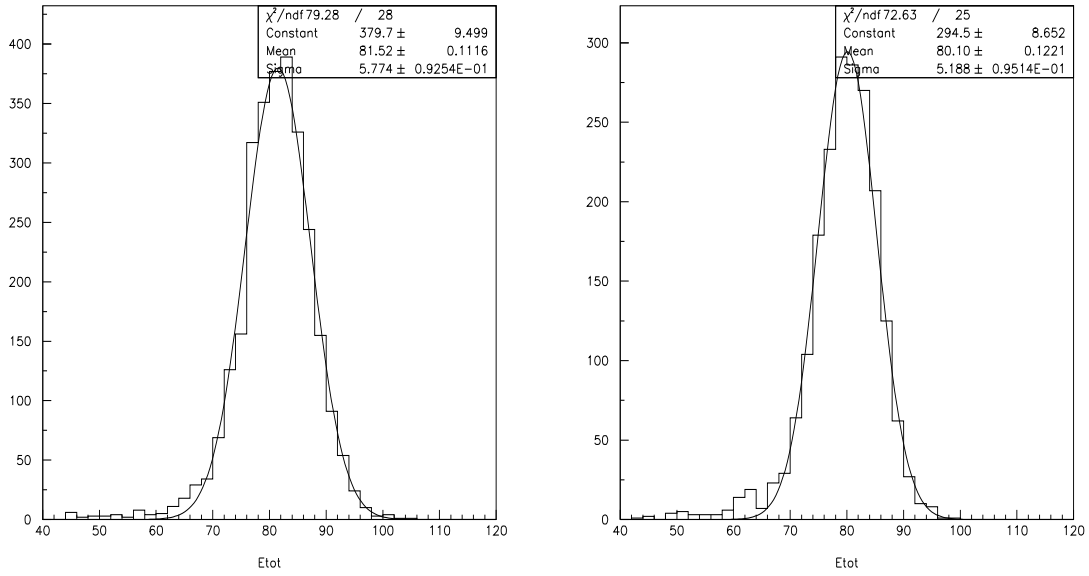

Figure 13: *Reconstructed energy using only 6 parameter and assuming no knowledge of the beam energy for pions at 80 GeV and η=-0.35. Left: test beam data. Right: Monte Carlo simulation.*

The mean, σ for η=-0.35 and resolution on the reconstructed energies are presented in tables 10 and 11. In figure 14 the linearity obtained by the "realistic" method is shown; the linearity remains as good as before. For test beam data the non-linearity ranges from 1.19% to 1.37% and from 0.48% to 0.85% for Monte Carlo simulation. The linearity given by the "realistic" mehtod is compared with the linearity obtained using the known beam energy. Also the *rms* for the Monte Carlo simulation is less than for the test beam data.

The resolutions obtained with the realistic algorithm, as we can see in figure 15 present a slight degradation with respect to the values given in the previous parametrization that uses the nominal beam energy. This result is unavoidable due to event-to-event fluctuations of hadronic showers. The figure shows that the degradation of the resolution is more pronounced at low energy, as expected from the energy dependence of σ/E. At high energy, the resolution for the test beam data is greatter than for the Monte Carlo simulation.

The final result for the test beam data and for the Monte Carlo simulation are shown in the table 12.

η=-0.35	Test Beam data		MC simulation	
N. E. (GeV)	μ (GeV)	σ (GeV)	μ (GeV)	σ (GeV)
20	19.51±0.06	2.22±0.06	20.58±0.05	2.16±0.04
50	50.22±0.09	3.93±0.07	50.87 ±0.07	3.82±0.07
80	81.79±0.11	5.69±0.09	79.44±0.09	5.16±0.09
100	101.5±0.1	6.86±0.10	98.80±0.11	5.92±0.11
150	154.7±0.3	9.27±0.22	149.9±0.2	8.07±0.16
180	186.8±0.2	11.07±0.16	177.2±0.2	9.19±0.22
300	311.7±0.4	18.01±0.27	297.2±0.5	13.13±0.49
400	406.7±0.5	26.45±0.45	395.7±0.6	15.72±0.60

Table 10: *Nominal energy, mean reconstructed energy and σ at various beam energies at η=-0.35 for test beam data and Monte Carlo simulation obtained assuming no knowledge of the beam energy.*

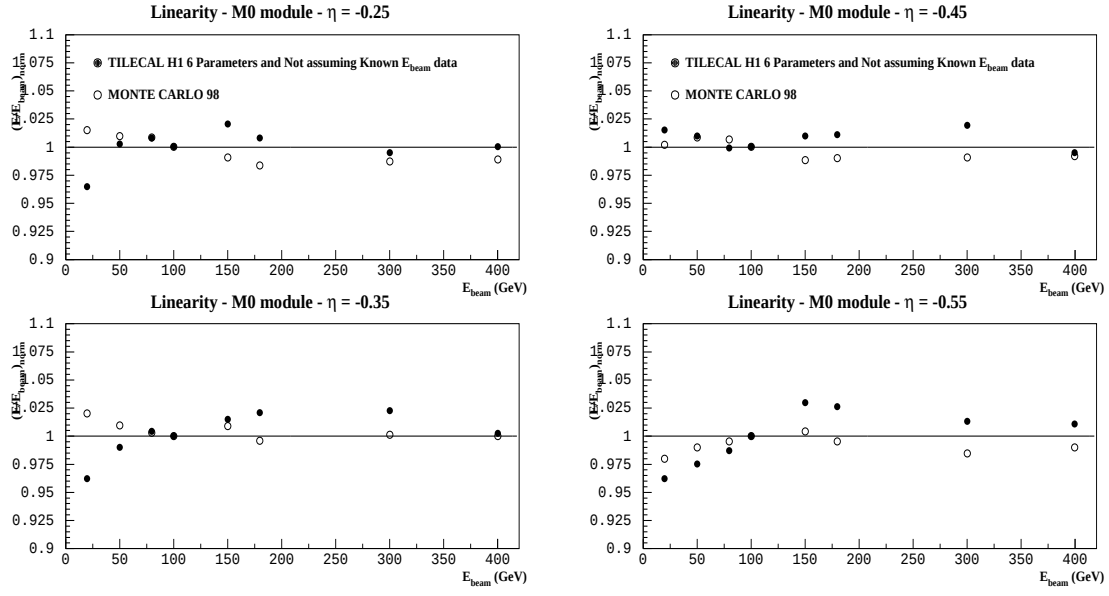

Figure 14: *Linearity plots without the beam energy knowledge for test beam data and Monte Carlo simulation. Left: For η=-0.25 (Top) and η=-0.35 (Bottom). Right: For η=-0.45 (Top) and η=-0.55 (Bottom).*

η=-0.25	Test Beam data	MC simulation
N. E. (GeV)	σ/μ(%)	σ/μ(%)
20	11.72±0.34	11.08±0.19
50	8.05±0.16	8.12±0.15
80	7.25±0.12	6.92±0.12
100	6.69±0.11	6.90±0.13
150	6.44±0.16	6.67±0.13
180	6.75±0.09	6.17±0.12
300	5.65±0.10	5.78±0.20
400	6.17±0.08	5.10±0.20
η=-0.35	Test Beam data	MC simulation
N. E. (GeV)	σ/μ(%)	σ/μ(%)
20	11.39±0.34	10.49±0.19
50	7.84±0.15	7.50±0.13
80	6.95±0.12	6.50±0.11
100	6.75±0.11	5.97±0.11
150	5.99±0.15	5.34±0.10
180	5.92±0.09	5.08±0.13
300	5.77±0.09	4.41±0.16
400	6.55±0.12	3.97±0.15
η=-0.45	Test Beam data	MC simulation
N. E. (GeV)	σ/μ(%)	σ/μ(%)
20	11.89±0.38	9.62±0.28
50	7.58±0.15	8.30±0.32
80	6.89±0.12	7.69±0.33
100	6.27±0.10	7.50±0.35
150	5.28±0.14	6.57±0.36
180	5.30±0.08	6.37±0.35
300	4.86±0.08	5.21±0.26
400	5.35±0.10	4.83±0.22
η=-0.55	Test Beam data	MC simulation
N. E. (GeV)	σ/μ(%)	σ/μ(%)
20	11.30±0.72	9.83±0.17
50	7.60±0.18	7.70±0.19
80	6.97±0.10	7.86±0.22
100	6.25±0.09	7.21±0.25
150	6.36±0.20	6.86±0.23
180	5.85±0.09	6.24±0.21
300	5.70±0.10	5.26±0.22
400	5.48±0.08	5.06±0.19

Table 11: *Nominal energy and resolution at various beam energies at four different η for test beam data and Monte Carlo simulation obtained assuming no knowledge of the beam energy.*

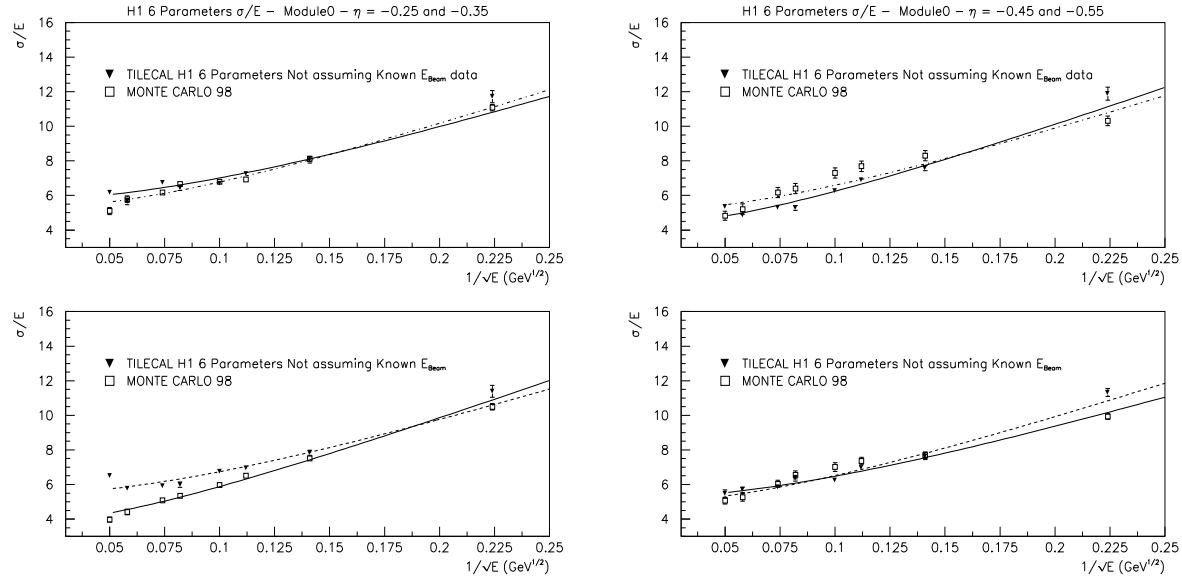

Figure 15: *Resolution plots without the beam energy knowledge for test beam data and Monte Carlo simulation. Left: For η=-0.25 (Top) and η=-0.35 (Bottom). Right: For η=-0.45 (Top) and η=-0.55 (Bottom).*

η	Test Beam data			MC simulation		
	a (%)	b (%)	c	a (%)	b (%)	c
-0.25	41.10	5.70	0.06	42.80	5.20	0.06
-0.35	40.80	5.30	0.06	45.70	3.70	0.06
-0.45	45.90	4.20	0.06	42.60	5.00	0.06
-0.55	43.20	4.80	0.06	39.00	5.10	0.06

Table 12: *Statistical (a), constant (b), and noise (c) terms at four different η for test beam data and Monte Carlo simulation obtained assuming no knowledge of the beam energy.*

4. The e/h and the e/π ratios

The responses obtained for e and π give the possibility to determine the e/h ratio, an intrinsic characteristic of a non-compensated calorimeter.

The present study corresponds to the data taken in 1997 for Extended Barrel and 1998 for Barrel Module 0.

For extracting the e/h ratio we have used the standard e/π method. The relation between the e/h ratio and the e/π ratio is:

$$e/\pi = \frac{e/h}{1 + (e/h - 1) \times 0.11 \times ln(E)} \tag{5}$$

where $0.11 \times ln(E)$ is the average fraction of the energy of the incident hadron into π^0 production [9].

Fig 16 and fig 17 show the e/π ratio as a function of the beam energy for BCN Extended Barrel module at four differents η values and for Barrel Module 0 at three differents η values. The response to pions relative to electrons is seen to increase with energy as expected, because the fraction of electromagnetic energy in a pion shower increases logarithmically with energy. The data have been fitted using equation (5) and a comparison with the Monte Carlo simulation for the Barrel Module at η=-0.45 has been done.

We could obtain four values for the e/h ratio. The results are presented in table 13 for the BCN Extended Barrel module and table 14 for the Barrel Module 0. The e/h ratio of a sampling calorimeter with an iron-scintillator ratio is expected to be > 1 for the conventional orientation of tiles perpendicular to incident hadrons. The tables show the results (e/h) as a function of η. In the BCN extended barrel module, the e/h value increases as the η increases, and for the Barrel Module 0 we obtain the same behaviour, except for η=-0.35. That could be explained by the different behaviour for the electron and pion responses as a function of η for the two calorimeter prototipes [10]. Deviations from e/h=1 contribute to the constant term in the energy resolution (see equation (2)). This constant term is about 3% for the BCN Extend Barrel [2] and about 5% for the Barrel Module 0.

The value of e/h=1.36 has been taken from previous precise studies, reported on the TDR [11]. At η=-1.1, for the BCN Extended Barrel, and η=-0.45, for the Barrel Module 0, there is a good agreement with this value, and also for the Monte Carlo simulation at the same η.

5.Comparison between Extended Barrel and Barrel Module 0

Two Extended Barrel Modules 0 were exposed in 1997 to the calibration beams, the first was built in Barcelona (BCN), Spain, and the other at Argonne, USA. This

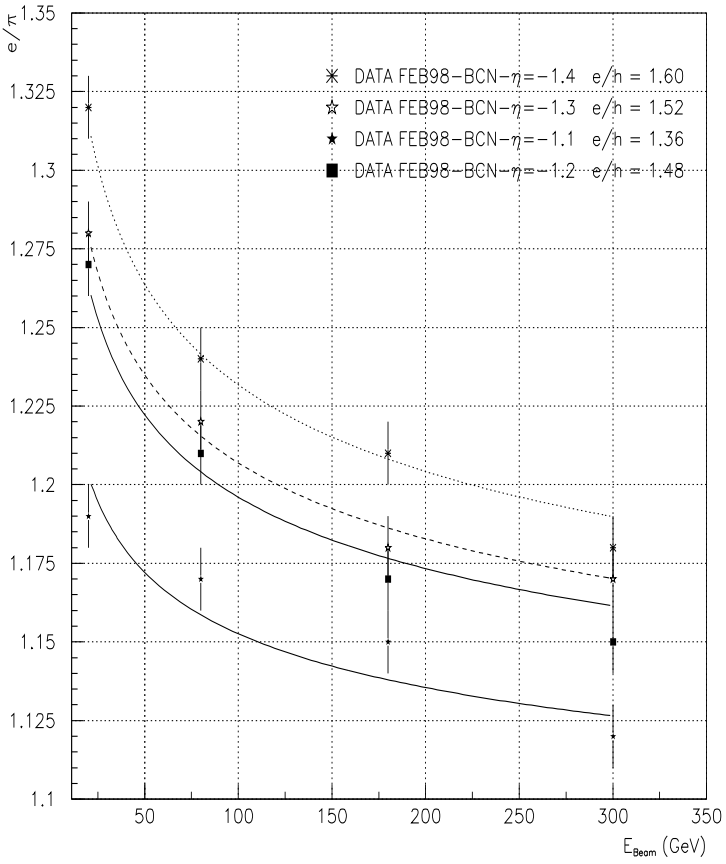

Figure 16: *The e/π ratio as a function of the beam energy for the BCN Extended Barrel module tested in the 1997 test beam at four differents η's. The lines are the fits of the equation (5).*

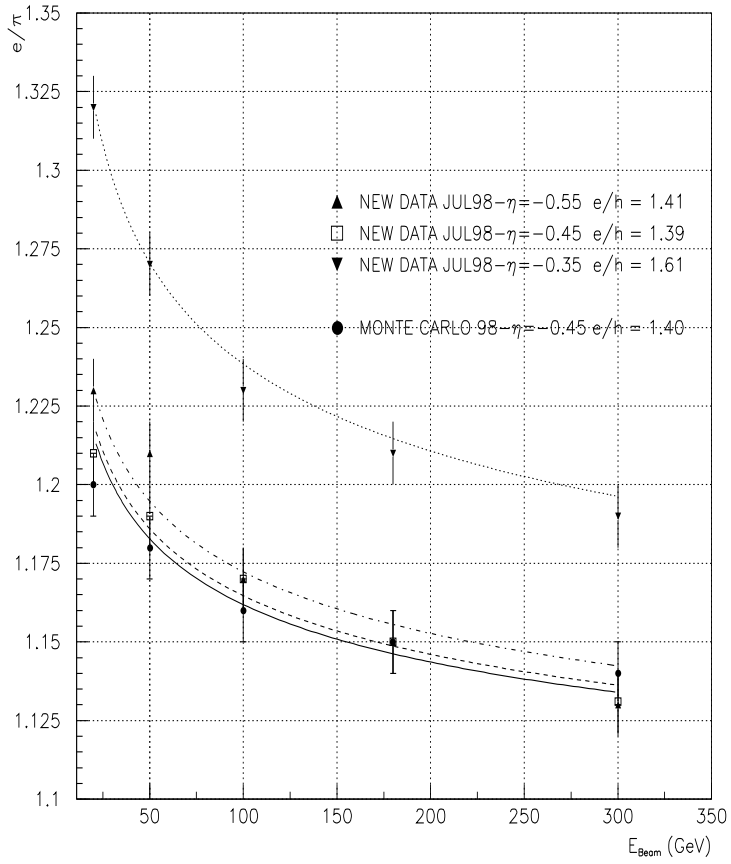

Figure 17: *The e/π ratio as a function of the beam energy for the Barrel Module 0 tested in the 1998 test beam at three different η's.The lines are the fits of the equation (5). The comparison for Monte Carlo data at η=-0.45 is also plotted.*

Module	η	e/h
BCN	-1.1	1.38 $\pm$0.013
BCN	-1.2	1.48 $\pm$0.014
BCN	-1.3	1.52 $\pm$0.015
BCN	-1.4	1.60 $\pm$0.016

Table 13: *The values of the e/h ratio for the BCN Extended Barrel module at four differents η's using the equation (5).*

Module	η	e/h
M0	-0.35	1.61 $\pm$0.015
M0	-0.45	1.39 $\pm$0.012
M0	-0.55	1.41 $\pm$0.012
M. C.	-0.45	1.40 $\pm$0.013

Table 14: *The values of the e/h ratio for the Barrel module 0 at three differents η's using the equation (5). Also the Monte Carlo simulation, at η=-0.45 is given in the table.*

test beam experience was also characterized by the cross talk effect. The H1 weighting technique has been studied in reference [2] for this test beam.

The table 15 shows the results obtained for the energy resolution after applying the H1 weighting technique to 1997 and 1998 test beam.

The average resolution for Extended Barrel is $\frac{\sigma}{E} = \frac{45.6\%}{\sqrt{E}} \oplus 3.0\% \oplus \frac{0.06}{E}$ and for the Barrel is $\frac{\sigma}{E} = \frac{42.7\%}{\sqrt{E}} \oplus 5.0\% \oplus \frac{0.06}{E}$. The statistical term is similar in the two cases and it is less than 50% (Hadronic calorimeter requirements [12]). The constant term is less in the Extedend Barrel than in the Barrel. As this term is related with the leakage, we can say that the Barrel Module 0 has more leakage (energy lost) than the Extended Barrel Modules 0 because the η values are higher than in the Barrel. For the Extended Barrel this term has a value around 3% (inside of the requirements) and for the barrel 5% (outside of the requirements).

The tables 16 and 17 show the *rms* for both Extended Barrel modules and for the Barrel Module 0 after applying the H1 weighting technique.

The average *rms* for Extended Barrel modules is 2.2% and for the Barrel module is 1.5%. The linearity requirements for the hadronic calorimeter come from the study of quark compositness where the jet energy scale has to be linear within 2% up to a transverse energy of 4 TeV. The *rms* from the Barrel is less than this value.

MODULE	η	a %	b %
BCN	-1.1	45.6 $\pm$ 0.7	2.71 $\pm$ 0.07
ANL	-1.1	47.8 $\pm$ 0.6	2.25 $\pm$ 0.06
BCN	-1.2	45.2 $\pm$ 0.7	3.10 $\pm$ 0.07
ANL	-1.2	43.7 $\pm$ 1.0	3.91 $\pm$ 0.07
M0	-0.25	41.1 $\pm$ 1.3	5.68 $\pm$ 0.08
M0	-0.35	40.7 $\pm$ 1.2	5.33 $\pm$ 0.08
M0	-0.45	45.9 $\pm$ 1.0	4.22 $\pm$ 0.08
M0	-0.55	43.2 $\pm$ 1.0	4.87 $\pm$ 0.10

Table 15: *The statistical and constant term from the resolution curves for the two Extended Barrel modules (test beam 1997) and for the Barrel module 0 (test beam 1998) at differents η's .*

η	-1.1	-1.2
BCN RMS (%)	1.2	3.0
ANL RMS (%)	1.8	2.9

Table 16: *The rms for both Extended Barrel modules and two values of η.*

6. Leakages parametrization

The aim of this section is to parametrize the leakages in order to improve the resolution. A prove that leakages exist is that in the Muon Wall there is signal.

A first idea was to apply cuts on the variable *MuBackHit* which represents the number of cells inside Back Muon Wall with signal greater than 0.7 mip. The figure 18 shows this variable for pion calibration beams 20, 100 and 400 GeV at η=-0.45.

At high energies the *MubackHit* variable can reach values up to 10, 12 and, 14, while at low energies only 1 or 2. This is because at high energies the leakage in the Barrel Module 0 is greater than at low energies. We can make a cut on this variable to obtain better results in the resolution, reducing the leakages contribution.

For this pourpose we have reconstructed the raw energy detected in the Barrel Module 0 for η=-0.45 and pion beam energy 400 GeV without and with cut in *MubackHit* (*Mubackhit*<3). This is shown in Figure 19. The resolution is better (evidently) when the cut is applied (from 5.7% to 5.0% for 400 GeV) but the number of entries has been strongly reduced (about 60% for 400 GeV) and also there is a clear reduction of the low energy tails. For this reason we decided to avoid the use of this cut.

An alternative is to parametrize the leakages with a gaussian. Figure 18 shows the

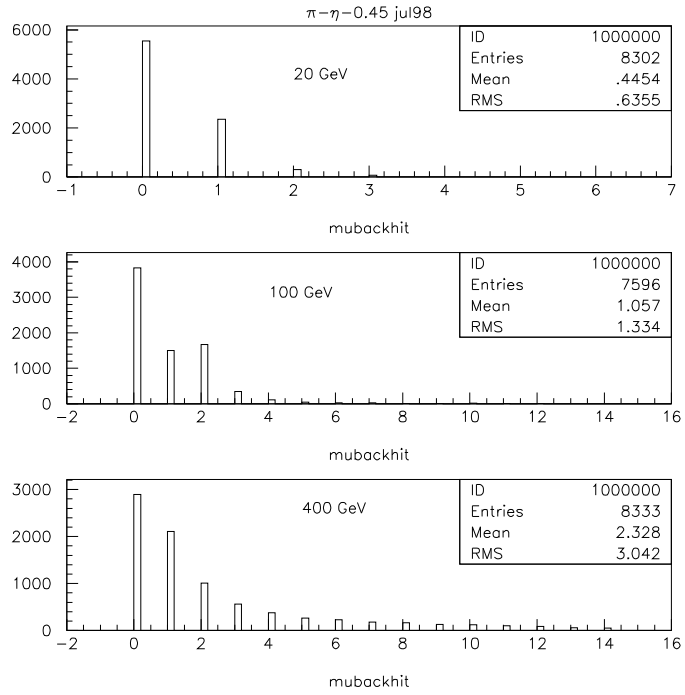

Figure 18: *Values of the MuBackHit variable for pion calibration beams at η=-0.45 and for three different energies.*

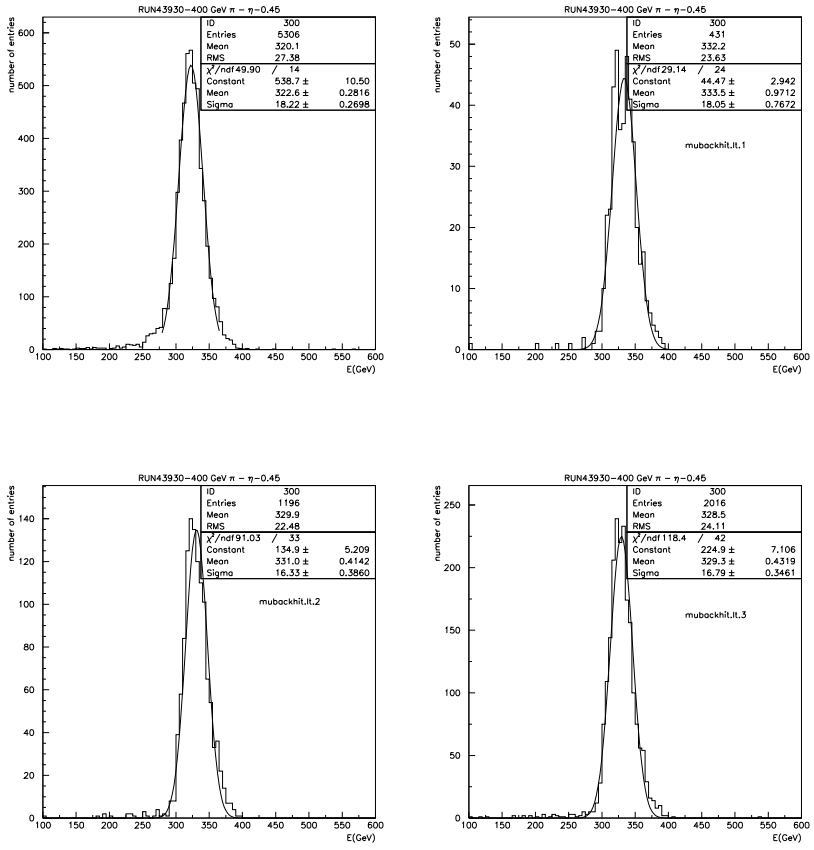

Figure 19: *Raw energy in the Barrel Module 0 for pions at 400 GeV and η=-0.45. Top left: without cut in MubackHit. Top right: with cut in MubackHit<1. Bottom left: with cut in MubackHit<2. Bottom right: with cut in MubackHit<3.*

η	-0.25	-0.35	-0.45	-0.55
RMS (%)	1.4	1.8	0.8	2.0

Table 17: *The rms for the Barrel Module 0 at four different η's.*

raw energy detected in the Barrel Module 0 for pion beam energy 400 GeV with cut in the *MubackHit* and parametrizing the leakages (low energy tails) with a gaussian. In both cases the resolution is 5.2% but if we fit the whole distribution with two gaussians (signal and leakage) all the physical entries are used.

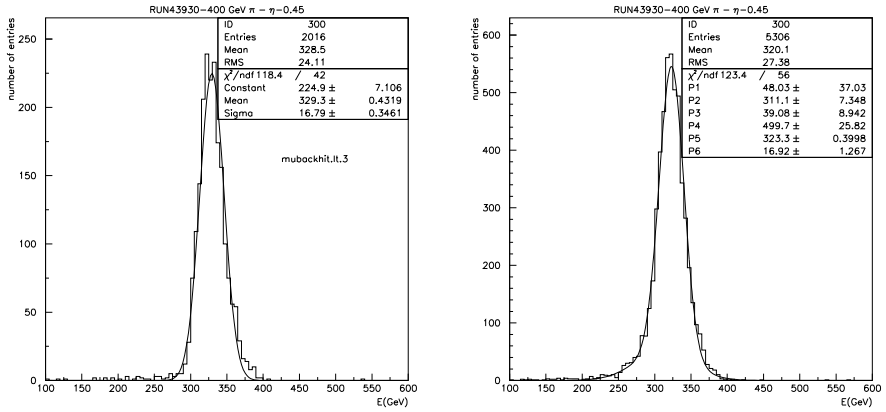

Figure 20: *Raw energy in the Barrel Module 0 for pions at 400 GeV and η=-0.45. Left: with cut in MubackHit. Right: Parametrizing the leakages with a gaussian.*

According with the expresion (1) we present the results of μ, σ , σ/μ in table 18 for $\eta = -0.45$ obtained from raw data and fitting with two gaussians. Also the plots of linearity and energy resolution fitting with a gaussian (top) and with two gaussians (bottom) can be seen in figures 21 and 22, respectively.

The *rms* for the linearity is 2.5% when only one gaussian is used in the fit and 2.8% when two gaussians are fitted. The *rms* are quite similar because the two precedures give practically the same value for the μ parameter.

For the resolution the fit results are presented in table 19, for the fit using one gaussian, two gaussians and H1 method.

The statistical term is similar in both cases (fit with one a two gaussians) but the constant term is better when we do the fit with two gaussians. This is because we have parametrized the leakages with a gaussian and the resolution has been calculated with the other gaussian. And besides, the constant term for the H1 method and for the fit with two gaussians is similar due to the fact that the weighting itself already

η=-0.45 N. E. (GeV)	μ (GeV)	σ (GeV)	σ/μ (%)
20	14.91 ± 0.02	2.06 ± 0.02	13.85 ± 0.13
50	38.62 ± 0.07	3.64 ± 0.05	9.42 ± 0.12
80	60.80 ± 0.46	4.63 ± 0.14	7.61 ± 0.23
100	77.98 ± 0.13	5.87 ± 0.37	7.52 ± 0.40
150	115.2 ± 0.7	6.73 ± 0.71	5.87 ± 0.60
180	143.4 ± 0.2	8.39 ± 0.22	5.85 ± 0.15
300	244.3 ± 0.3	14.83 ± 0.31	6.07 ± 0.13
400	323.3 ± 0.3	16.92 ± 0.90	5.23 ± 0.30

Table 18: *Nominal energy, mean reconstructed energy , σ at various beam energies at $\eta = -0.45$ obtained from raw data and doing the fit with two gaussians.*

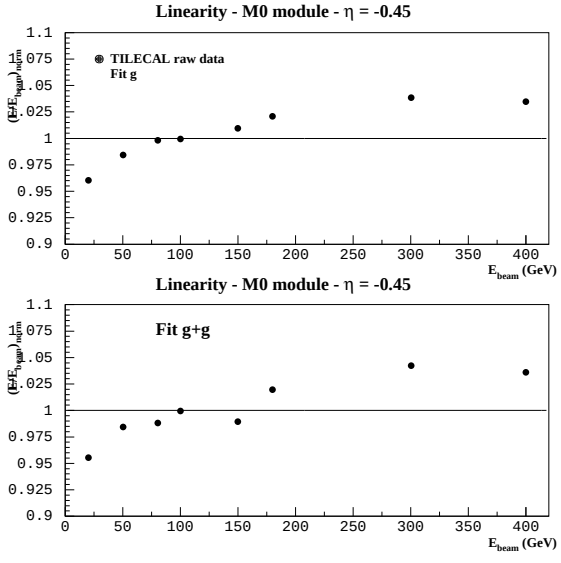

Figure 21: *Linearity of raw data doing the fit with a gaussian (top) and with two gaussians (bottom) for $\eta = -0.45$.*

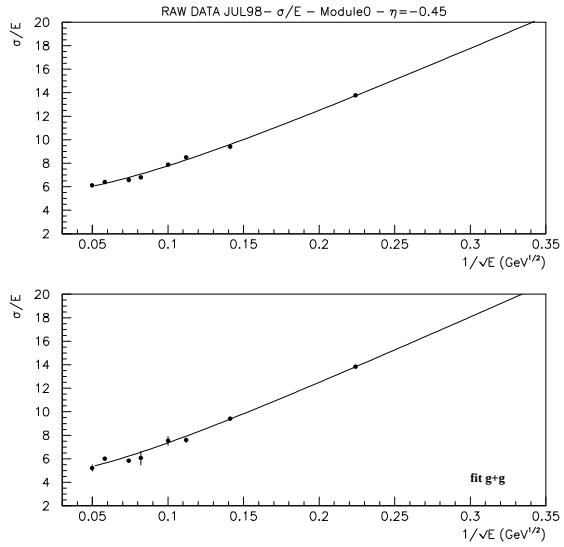

Figure 22: *Energy resolution of raw data doing the fit with a gaussian (top) and with two gaussians (bottom) for* $\eta = -0.45$.

provides a reduction of the low energy tails (see figure 13).

η	Fit (1 gaussian)			Fit (2 gaussians)			H1		
	a (%)	b (%)	c	a (%)	b (%)	c	a (%)	b (%)	c
-0.45	56.50	5.35	0.06	58.30	4.49	0.06	45.10	4.15	0.06

Table 19: *Statistical (a), constant (b), and noise (c) terms for* $\eta = -0.45$ *doing the fit with a guassian , two gaussians and applying the H1 method.*

7. Conclusions

In this study we have proved that the linearity and resolution of the Barrel Module 0 improve using the H1 method. Also the good agreement between the Monte Carlo simulation and the Test beam data after applying H1 weighting technique for the four different values of η has been seen.

Respect to the linearity, using Lagrange multipliers we found a very good linear response over the range of energies studied, because 112 weights have been used for each module. With the parametrization of these weights using a total of 6 constants and assuming no knowledge of the particle energy the linearity is degraded but the average *rms* is around 1.5% and therefore inside the requirements. The linearity for the Monte Carlo simulation is better than the test beam data but at high energies the hadronic shower simulation is insufficient and the shower description became quite far away from reality.

For the resolution, the use of all those weights improves significantly the resolution respect to the raw data algorithm. As expected, the resolution degrades somewhat when no knowledge of the particle energy is assumed, been better than the obtained with the other methods. The statistical and the constant terms are very similar for the Monte Carlo simulation and test beam data having a mean value around 43% and 5%, respectively.

The *e/h* ratio is around 1.4 and is compatible with the one obtained in other studies. There is a good agreement between the test beam data and the Monte Carlo simulation.

Respect to the comparison between the Extedend Barrel modules 0 and the Barrel module 0, the statistical term from the energy resolution is similar but the constant term is greater in the Barrel than in the Extended Barrel, therefore the Barrel Module 0 has more leakage because the η values are smaller than in the Extended Barrel. On the other hand, the *rms* is less in the Barrel than the Extended Barrel and the *e/h ratio* is very similar for both calorimeter prototipes.

To parametrize the leakages in order to obtain better resolution, we decided to avoid the use of the Back Muon Wall cut because it reduces the number of entries around 60%. Instead of a fit with two gaussians gives the same resolution and uses all physical entries. Moreover the weighting technique already provides by itself a reduction of the low energy tails.

Acknowledgments

This work is the result of the efforts of may people from the ATLAS Collaboration. The authors are grateful to B. Di Girolamo for his attention, support and suggestions on this work. We want to thanks M. Nessi, R. Stanek, E. Higón and F. Camarena for many valuables comments.

References

[1] M.P. Casado et al., ATLAS Internal Note TILECAL-NO-75 (1996).

[2] F. Camarena et al., ATLAS Internal Note TILECAL-NO-99-001 (1999)

[3] Geant-Detector Description and Simulation Tool, CERN Program Library, Geneva, Switzerland, Oct. 1994.

[4] DICE manual Version 0.10, CERN, Switzerland, Feb.1995

[5] M. Nessi et al., ATLAS Internal Note SOFT-NO-16 (1994)

[6] C. Zeitnitz et al., The GEANT-CALOR Interface user's guide, CERN, Aug. 1995

[7] C. W. Fabjan, CERN-PPE-94-61 (1994).

[8] H1 Calorimeter Group, W. Braunschweig et al., DESY Internal report, DESY 89-022 (1989).

[9] R. Wigmans, NIM A265 (1998) 273..

[10] Y. A. Kulchitsky et al., ATLAS Internal Note TILECAL-99-002 (1999).

[11] Tile Hadronic Calorimeter TDR, CERN/LHCC 96-42 (1996).

[12] Calorimeter Performance, CERN/LHCC 96-40 (1997).